

CAMERA AND VISUAL VEILING GLARE IN HDR IMAGES

John J. McCann and Alessandro Rizzi

McCann Imaging, Belmont, MA 02478, USA

Dip. Tecnologie dell'Informazione - Università degli Studi di Milano, 26013 Crema (CR), Italy

Keywords: HDR imaging, veiling glare, calibration of multiple exposure techniques, spatial algorithms, Retinex, ACE

ABSTRACT

High-dynamic-range (HDR) images are superior to conventional images. The experiments in this paper measure camera and human responses to calibrated HDR test targets. We calibrated a 4.3-log-unit test target, with minimal and maximal glare from a changeable surround. Glare is an uncontrolled spread of an image-dependent fraction of scene luminance in cameras and in the eye. We use this standard test target to measure the range of luminances that can be captured on a camera's image plane. Further, we measure the appearance of these test luminance patches. We discuss why HDR is better than conventional imaging, despite the fact the reproduction of luminance is inaccurate.

Keywords: HDR Imaging, veiling glare, tone-scale maps, Retinex, ACE.

1. INTRODUCTION

This paper is the second of a pair of our papers on HDR imaging. The prior paper¹ reviews the long history of HDR imaging from Renaissance paintings to modern digital imaging. This paper measures the effects of veiling glare on camera image capture and the appearance of the same scenes viewed by humans.

Recently, multiple exposure techniques² have been combined with LED/LCD displays that attempt to accurately reproduce scene luminances.³ However, veiling glare is a physical limit to HDR image acquisition and display. We performed camera calibration experiments using a single test target with 40 luminance patches covering a luminance range of 18,619:1 (4.3 log units). Veiling glare is a scene-dependent physical limit of the camera and lens.^{4,5,6,7} Multiple exposures cannot accurately reconstruct scene luminances beyond the veiling glare limit.

Human observer experiments, using the same targets, show two independent and opposing visual mechanisms. Intraocular veiling glare reduces the luminance range on the retina while physiological simultaneous contrast⁸ increases the apparent differences.

There must be reasons, other than accurate luminance, that explain the improvement in HDR images. The multiple exposure technique significantly improves digital quantization. The improved quantization allows displays to present better spatial information to humans. When human vision looks at high-dynamic range displays, it processes scenes using spatial comparisons.

2. HDR TEST TARGETS

While ISO 9358:1994⁹ provides a standard to compare different lenses and apertures; we wanted to measure the effects of veiling glare on HDR imaging. We used a single calibrated test target with 40 test luminance sectors (dynamic range = 18,619:1). Nearly 80% of the total target area was an adjustable surround; 20% of the area was luminance test patches. Using opaque masks to cover the surrounding portions of the scene, we photographed three sets of HDR test scenes with different amounts of glare. The experiment compares camera digits with measured scene luminance over a very wide range of luminances and exposure times. This experiment measured the extent that veiling glare distorts camera response in situations common with HDR practice.

In 1939, Kodak patented the Projection Screen Print Scale for making test prints¹⁰. It is a circular step wedge with 10 pie-shaped wedges, each with a different transmission. The range of transmissions was 20:1. After focusing a negative in an enlarger on the print film plane, darkroom technicians would place this scale on top of the unexposed print film in the dark. The wedges transmitted 82%, 61%, 46%, 33%, 25%, 17%, 14%, 9%,

8% and 4% of incident light so as to make a quick and accurate test print to select the optimal print exposure. We used these Scales to make 10 different test luminance sectors.

The components of our test display are shown in Fig 1. The display is made of transparent films attached to a high-luminance light-box. There are four Kodak Print Scale transparencies mounted on top of 0.0 (ScaleA), 1.0 (B), 2.0 (C), and 3.0 (D) N.D. filters. The 40 test sectors are constant for both minimal (*4scaleBlack*) and maximal (*4scaleWhite*) glare so that both targets have the same range of 18,619:1. For minimal glare, we covered all parts of the display except for the pie-shaped projection scales with an opaque black mask (*4scaleBlack*). For maximal glare, the opaque black mask was removed so that the zero-glare surround was replaced with maximal glare (*4scaleWhite*). The diagonal line in *4scaleWhite* is an opaque strip in front of the display. To further reduce glare, we covered the background and scales A, B and C, leaving only the light coming from scale D (*1scaleBlack*) with a 20:1 range.

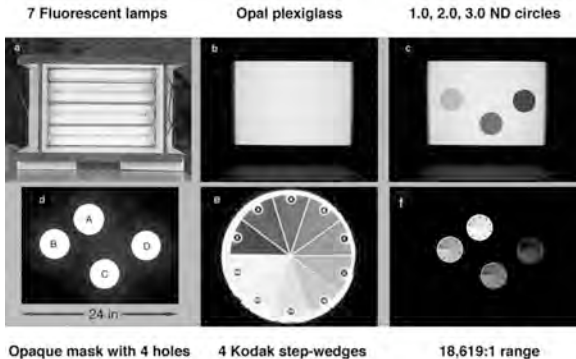


Figure 1a shows the light source made of 7 fluorescent tubes (20W). Figure 1b shows an opal-Plexiglas diffuser placed 15 cm in front of the lamps. Figure 1c shows the addition of 3 circular neutral density filters attached to the Plexiglas with densities of 1.0, 2.0, and 3.0. Figure 1d shows an opaque mask that covered the entire lightbox except for four circular holes registered with the N.D. filters. Figure 1e shows an enlarged view of a single Kodak Projection Print Scale. Figure 1f shows the assembled *4scaleBlack* target with a dynamic range of 18,619:1 [2049 to 0.11 cd/m²]. Using opaque black masks, the luminance of each sector was measured with a spot luminance meter (Konica-Minolta LS-100C), one wedge at a time in a dark room.

3. CAMERA VEILING GLARE LIMITS

We made separate sets of measurements first with a digital camera, then with a 35mm film camera using both slope 1.0 slide duplication and conventional negative films. We also used a lensless pinhole camera. We used all three HDR calibrated targets to measure the camera response. With the *1scaleBlack* target we measured the camera response using only the lowest luminances with a 20:1 range. With the *4scaleBlack* target we measured the camera response using a high

display range of 18,619:1 with minimal glare. With the *4scaleWhite* target we measure the camera response using the same display range with maximal glare.

3.1 Digital Camera Response

We made photographs using a typical compact, high-quality digital camera (Nikon Coolpix 990) with manual, mid-range aperture (set to f 7.3) and exposure time controls. The experiment photographed 3 sets of records shown in Figure 2.

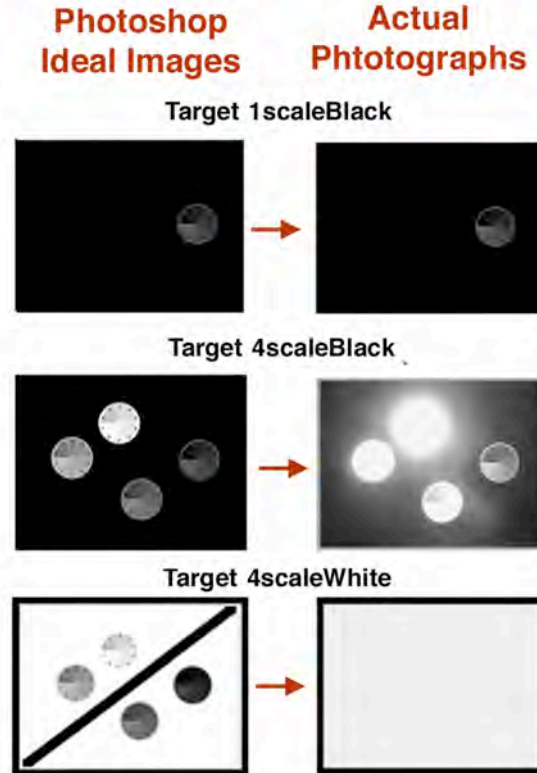


Figure 2 (left) shows ideal synthetic Photoshop images of the three test targets and (right) shows the actual 16 sec exposures of the test target acquired with the digital camera. The 16-sec exposure is optimal for recording the luminances of the lowest luminance scale D. The punctual luminance values at each wedge sector remain unchanged in the three scenes. A 16 sec exposure of the *1scaleBlack* target shows a typical camera response with digits from 37 to 201. Veiling glare has a small, but significant incremental effect on camera response to *4scaleBlack*. Glare from the other test sectors has increased camera digits. The darkest sector digit increased from digit 37 to 98. Veiling glare overwhelms the camera response to *4scaleWhite*. All pixels have the saturated maximum value (242).

The intent of multiple exposures in HDR imaging is to calculate a new image with a significantly greater dynamic range record of the scene.² The idea is simply to assume that scene flux [(cd/m²) * sec] generates a unique camera digit. Longer exposures collect more scene photons, and can move a dark portion of the scene up onto a higher region of the camera response function. This higher exposure means that the darker portions of the scene have better digital segmentation, more digits for better quantization of luminances. Digital HDR

multiple-exposure techniques^{11,12,13,14,2} claim to extend the cameras range by calibrating flux vs. camera digit. Debevec and Malik make the specific argument that calculations using multiple exposure data derive high-dynamic-range scene luminance. For reference, this technique will be described below as Multiple Exposure to Scene Luminance (ME2SL). This is to distinguish this use of multiple exposures from others described in the previous paper.¹

Given our calibration measurements of the test target scene, we can paste together in Photoshop the desired ideal image. Dividing the 2049 to 0.11 luminance range into 256 levels we get an 8 (cd/m^2) increment per gray level. These synthetic ideal images are shown in the left column of Figure 2. The right column shows actual photographs. The differences between ideal and actual images are due to unwanted veiling glare. The results in Figure 2 show that glare can be substantial.

We measured the veiling glare's influence with 16 shots taken with variable exposure times and the same f-7.3 aperture (Figure 3). We selected this camera because it has manual controls for both aperture and time of exposure. The *1scaleBlack* photographs have the lowest veiling glare and provide an accurate measure of the camera sensor response function. The only sources of glare are the test patches themselves (range 20:1). The camera response is the average digital value (from 491 pixels) calculated in Photoshop for a circular area falling inside the pie shaped luminance sector.

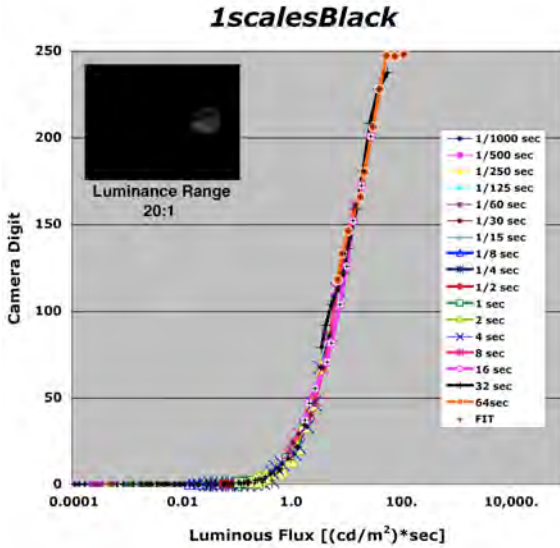


Figure 3 plots *1scaleBlack* (range 20:1) camera digits. It shows the desired coincidence of camera digits and flux. The curve provides us with an accurate camera response function. The sensor digits saturate at 247 with a flux of $78.4 \text{ sec} \cdot \text{cd}/\text{m}^2$; at digit 1 the flux is $0.107 \text{ sec} \cdot \text{cd}/\text{m}^2$. The camera dynamic range is 731:1, or 2.9 log units. The black + symbols plot lookup table data derived from the average measured digital data. This lookup table assigns an average luminance value to each digital value from 0 to 255. This lookup table is the camera response function.

The degree of overlap of multiple exposure responses with flux is possible because of the accuracy of the camera's exposure-time mechanism and the level of veiling glare found in the 20:1 test target. The Multiple Exposure to Scene Luminance (ME2SL) technique works well in these conditions. The data in Figure 3 is plotted as flux (luminance * time) because that is related to the total number of photons falling on the camera's CCD sensor. We cannot derive actual photon counts without detailed knowledge of the cameras spectral responses, and anti-blooming, noise reduction and tone scale circuits. Nevertheless, we can plot (measured luminance*exposure time) to define the scene flux before interaction with the camera. The results in Figure 3 provide a consistent measure of camera response and a lookup table that allows us to convert camera digit to estimated scene luminance. This estimate is accurate as long as the ME2SL technique is error free, as shown in Figure 3.

In *4scaleBlack* the camera's digit responses to four 10-step scales attempt to capture a combined scene dynamic range of 18,619:1 (Figure 4). This target measures the minimum glare for a scene with this range, because it has an opaque black surround. The only source of glare is the test patches that vary from 2094 to $0.11 \text{ cd}/\text{m}^2$.

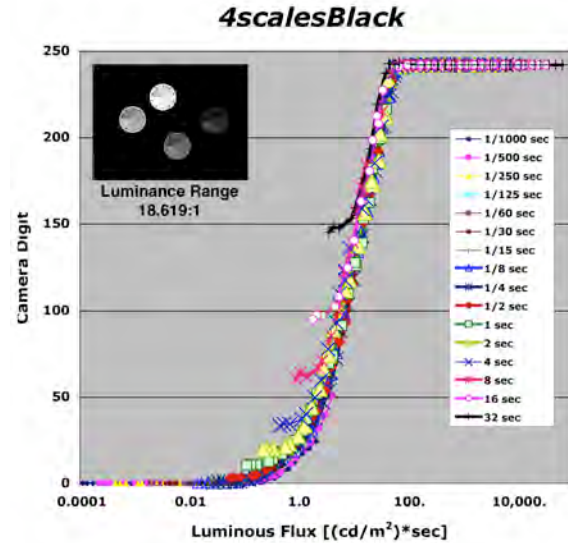


Figure 4 plots *4scaleBlack* (range 18,619:1) camera digits. It shows the minimal effects of glare for this range and configuration using a black surround between test scales. For an optimum exposure (1/2 sec) the sensor digits saturate at 242 with a flux of $119 \text{ sec} \cdot \text{cd}/\text{m}^2$; at digit 11 (departure from camera response curve) with a flux of $0.84 \text{ sec} \cdot \text{cd}/\text{m}^2$. The glare limited dynamic range is 141:1, or 2.2 log units for this exposure. The effects of glare are seen as departures from a single camera function in low-luminance sectors.

The data from Figure 4 shows that camera digit does not predict scene flux because the data for scale D fails to fall on the single camera response function measured in Figure 3. The same scene luminance generates different (exposure-dependent) digits. This is important because this display was intended to measure the minimal glare for an 18,619:1 scene. Despite the fact that 80% of the target area is glare free, we measure a problem with the ME2SL technique.

When we removed the black mask covering the lightbox in the background, we go to the situation with maximal veiling glare (*4scaleWhite*). Nearly 80% of the pixels are making highest possible contribution to veiling glare (Figure 5).

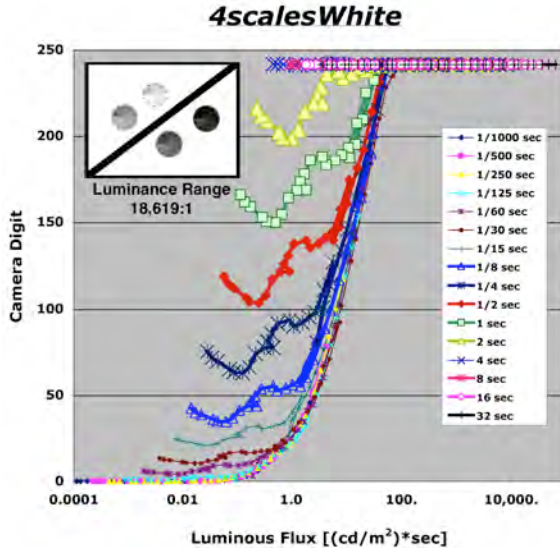


Figure 5 shows the camera digits from 16 different exposure times for the *4scaleWhite*, the high-glare target. The many large departures from a single line are due to scene-dependent glare. All departures from the camera response function (Figure 3) are errors in the ME2SL technique.

Figure 5 shows that the influence of glare is dramatic. For Scales C and D camera digits are controlled as much by glare as by luminance.

The data from all three sets of photographs are different. Data from *1scaleBlack* (Figure 3) provides a single camera sensor response function. Camera digit correlates with scene flux. Data from *4scaleBlack* shows a lack of correlation for low luminances at some exposures. Data from *4scaleWhite* shows that glare corrupts camera digit correlation with scene flux. This is a major problem for ME2SL technique. It works well only when veiling glare is low. Veiling glare is scene dependent.

Camera digits from multiple exposures cannot provide a trustable means of measuring HDR scene flux. Camera digits cannot accurately record HDR scene flux because of glare. Veiling glare is scene dependent. We also have performed tests using different cameras, and

various changeable lenses, and we obtained similar results.

We took the data of Scale D from *1scaleBlack* to generate a lookup table that describes camera digit as a function of flux and its inverse (See FIT in Figure 3). We then used this camera response lookup table to convert the camera digits from *4scaleBlack* and *4scaleWhite* to calculated flux. We took the ratio of camera-estimated flux to actual measured flux. This ratio is a measure of ME2SL error of each target sector. If the camera digit accurately predicted scene flux then this ratio equals 1.0. Ratios greater than 1.0 measure the magnitude of errors introduced by glare. and Figure 6 plots these ratio values vs. scene luminance.

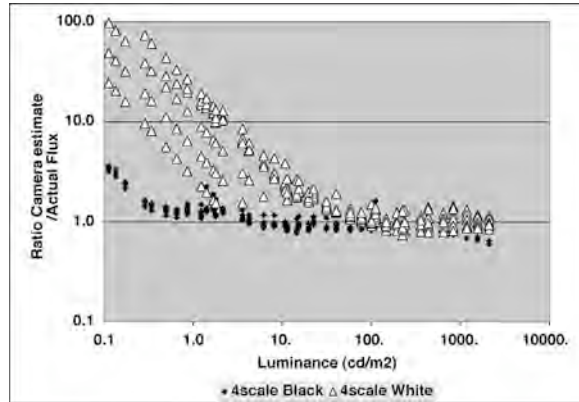


Figure 6 plots the ratio of camera-estimated flux to actual flux for *4scaleBlack* and *4scaleWhite*. If camera digit accurately measures scene luminance (ME2SF), then all the data must fall on a horizontal line (ratio = 1.0). The results support that hypothesis from 50 to 2048 cd/m² (range 40:1). Below 50 cd/m², the *4scaleWhite* data show that veiling glare distorts the ratios, and hence the luminance estimates. The same is true for *4scaleBlack* below 3 cd/m². The target has a range of 4.3 log units. Camera estimates of luminance are accurate on average over 2.8 log units with black surround (minimal glare) and 1.6 log units with white surround (maximal glare).

The *4scaleBlack* target has no glare from 77% of the scene area, yet shows worst-case errors as large as 300% distortions. The *4scaleWhite* target (maximal glare) shows 10,000% errors. If we hypothesize a variety of different surrounds to substitute for the all white, or all black surround, all possible luminance backgrounds, around Scales A, B, C, and D, will fall in between the white and the black data sets. Substituting all possible surrounds for the white, and the black, will generate veiling glare luminance estimate errors between 300% and 10,000% for this scene.

The data from *4scaleWhite* in Figure 6 shows a series of parallel lines deviating from the slope 0.0. There show different, large glare distortions for the same luminance depending on exposure. This adds *exposure* to the list of physical attributes controlling glare. The others are: scene, camera body, lens and aperture size. The ME2SL technique is subject to glare limits that are difficult to

estimate for any scene, camera, lens, aperture, and exposure.

3.2 Duplication Film-Camera Response

We made another set of photographs with a typical high-quality 35 mm film camera (NikonFM with a Nikkor 50mm 1:2 lens) using Kodak Slide duplication film. This follows the single exposure HDR capture technique described by McCann¹⁵ in tutorials at Siggraph conferences in 1984 and 1985. Slide duplication film has slope 1.0 on a log exposure vs. log luminance plot. In other words, output luminance is equal input luminance. Since it is a color film it can be scanned for color and does not require calibration to remove the color masks found in color negative film. Here we use multiple exposures to capture both 18,619:1 displays (*4scaleBlack* and *4scaleWhite*). The exposed film was developed with standard E6 process. All exposures were mounted in a single 35 mm film holder so that all images were scanned at the same time with the same scanner settings. The scanner was an Epson Perfection Photo with calibration for E6 films. Figures 7 and 8 plot scanned positive film digit vs. log flux.

Figure 7 data show that this particular camera-film-scanner system has less veiling glare than the digital camera in section 3.1.

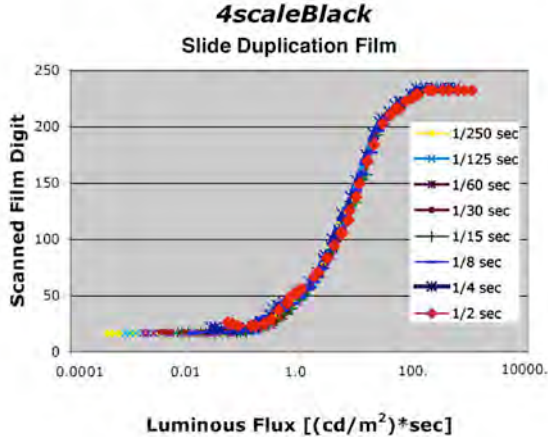


Figure 7 plots scanned film digit vs. luminous flux for 8 exposures ranging from 1/250 sec to 1/2 sec for *4scaleBlack*. The data from the 8 different exposures superimpose to form a single function, except for the very lowest luminance sectors.

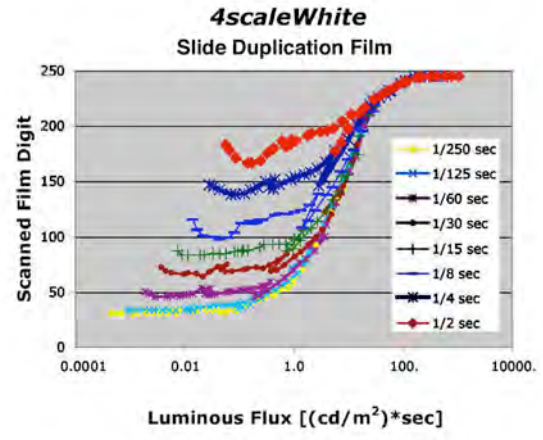


Figure 8 plots data for *4scaleWhite*. Here the white surround adds veiling glare to generate 8 different response functions. \square

Although there may be small differences between this data and the digital camera's response in 4.1, the same scene-dependent glare dominates both results.

3.3 Negative Film-Camera Response

We made another set of photographs with the same NikonFM camera using Kodak Max 200 negative film. The exposed film was developed with standard C41process. Again, all exposures were mounted for a single scan at the same time with the same scanner settings. The scanner was an Imacon Flexlight Precision with calibration for C41 films.

First, we used 7 different exposures to measure the camera-film-scanner process using the low glare 20:1 single scale (*1scale Black*). The gray triangles in Figure 9 plot the combined response of film, camera, development process, and film scanner (called Negative).

We then photographed *4scaleBlack* at and *4scaleWhite*, using the same single exposures to capture the 18,619:1 displays. In the case of the white surround, the gray scales had high digital values, covering less than 50 digits. We made an additional single exposure called *4scaleWhite2* negative with shorter exposure time. This scanned film had a digit range of 150, allowing better quantization of the scene.

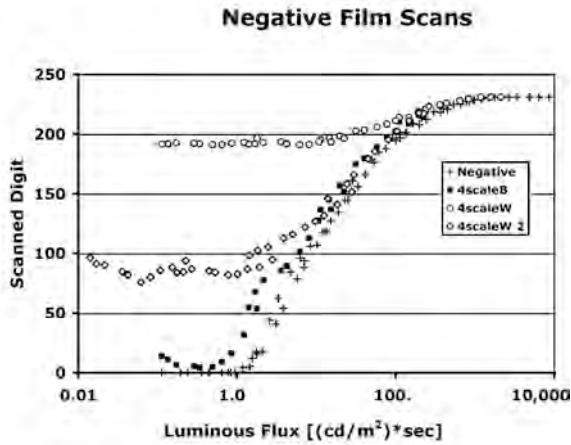


Figure 9 plots scanned single negative digits vs. log luminous flux for three targets. The *4scaleBlack* data (+ symbol) plots data from 7 negatives with different exposures. The + symbols report the response of the camera-film-scanner process with the lowest level of glare (20:1 target). It shows that the negative process can accurately record fluxes from 2639 to 0.24 sec*cd/m². The *4scaleBlack* (black squares) and *4scaleWhite* (white circles and diamonds) targets measured negative responses with single exposures. The single exposure curve from *4scaleBlack* saturates at 1181 sec*cd/m² and inverts at 0.34 sec*cd/m². The inversion is caused by glare that limits usable range. There are two different single exposures for *4scaleWhite* target; one is 8 times longer than the other. The data from *4scaleWhite* (white circles) saturates at 1,181 cd/m² and inverts at 6.17 cd/m². The curve from *4scaleWhite2* (white diamonds) has a maximum digit at 2094 cd/m² and inverts at 6.17 cd/m².

Figure 9 shows that the negative-camera-scanner process can accurately record fluxes from 2639 to 0.24 sec*cd/m² (dynamic range of 11,100:1, or 4.05 log units) [See Table 1]. The single exposure data from *4scaleBlack* show a small effect of glare from the addition of 30 higher luminance test pie-shaped areas. This glare reduces the dynamic range of the image in the camera to 3.5 log units. The glare from the white surround in *4scaleWhite* and *4scaleWhite2* reduces the dynamic range of the image measurements to 2.3 and 2.5 log units.

The fact that the dynamic ranges for the two exposures of the *4scaleWhite* target are almost the same is important. Their response curves in figure 9 are very different. The *4scaleWhite* scanned digits have a max of 231, and a min of 191. The *4scaleWhite2* scanned digits have a max of 223, and a min of 94. The range of digits representing the scene is only of secondary importance. The range of digits describes the number of quantized levels used to represent the image. It controls discrimination, but does not control the dynamic range of the image.

Target	Max Flux	Min Flux	Range	Log Range
Negative	2639.0	0.24	11,100	4.05
4scaleB	1181.4	0.34	6,345	3.54
4scaleW	1181.4	6.17	192	2.28
4scaleW2	2094.2	6.17	340	2.53

Table 1 shows the range limits of the negative film plotted in Figure 9. It lists the maximum flux below system saturation (Max Flux), the minimum flux above digit reversal from glare (Min Flux), the dynamic range equal to Max Flux / Min Flux ratio (Range), and log ratio (Log Range).

There is an interesting characteristic of scanned negatives. The lowest density film (highest transmission) response measures the lowest scene luminance levels. These areas send the most light to the scanner and have the best signal-to-noise scanner response. As shown in Figure 9, there is a long "toe" region that stretches from 100 to 10000 sec*cd/m². Over that 2 log units scene range the scanned digits are all above 200. Although the digital quantization is poor, the sampling (average digital value) discrimination is excellent because of the strong signal read by the scanner.

Conventional negative film can capture a greater range of luminances than falls on the camera image plane from these targets. The dynamic range of a single exposure negative-film-scanner process exceeds the glare limited *4scaleBlack* scene by 0.5 log units and glare limited *4scaleWhite* scene by 1.6 log units (Table 1). Multiple exposures with negative films serve no purpose. The glare-limited ranges of the camera and these HDR scenes are smaller than the film system range.

L. A. Jones and H. R. Condit¹⁶ measured the luminance range in 128 typical outdoor photographic scenes. They reported a minimum range of 27:1; the maximum was 750:1; and the average was 160:1. Nevertheless, one can increase the scene range by including the light source and specular reflections. The above data from Section 3 suggests that in high, and in average glare scenes, the glare-limited image dynamic range on the film/CCD image plane will be less than 3.0 log units. Only in special cases, very low-glare scenes, will the image plane's dynamic range exceed 3.0. The data here show how well the designers of negative films did in optimizing the process. They selected the size distribution of silver halide grains to make the negative have a specific dynamic range, around 4.0 log units. Thus, single-exposure negatives capture the entire range

possible in cameras, with low glare scenes. For most scenes this image capture range provides a substantial exposure latitude, or margin of exposure error. After reading the papers of C. K. Mees, L. A. Jones, and H. R. Condit, it is easy to believe that this fact is not a coincidence.^{16,17,18}

3.4 Pinhole-Camera Response

Sowerby, in his *Dictionary of Photography*¹⁹ discusses the reflection of light in lenses as the diversion of an appreciable portion of the incident light from its intended path. The small percentage of light reflected from each air-glass surface is called a parasitic image. Parasitic images that are completely out of focus give rise to a general fog that limits the dynamic range of the image falling on the film plane. The actual *4scaleB* image (Figure 2) shows a magnified inverted in-focus parasitic image, as well as, the out-of-focus fog from other parasitic images. Multiple exposures improve the digital quantization and thus the sensor's performance. Nevertheless, multiple exposures have no effect on the dynamic range of the image falling on the sensor. The digital camera used in Section 3 has 9 elements and 153 parasitic images.²⁰ The film camera used in Sections 3.2 and 3.3 has 7 elements and 91 parasitic images.¹⁸

An interesting problem is to measure the dynamic range of images made with a lensless pinhole camera.²¹ We made a pinhole out of soft black plastic, counter bored with a 1 cm drill and pierced with a needle. The pinhole was slightly elliptical. The average diameter was 376 microns (392 by 362). It was placed 50 mm from the film plane. Each point source in the scene is diffracted by the pinhole. Figure 10 shows the Airy pattern formed by diffraction.²² The major lobe (peak to first minimum), called Airy's disc, is 83.7% of the light falling on the image plane.²³ The diameter of that lobe in 550nm light in this camera is 0.178 mm. The remaining 16.3% of the light is diffracted outside the disc to form a diffracted fog that limits dynamic range.

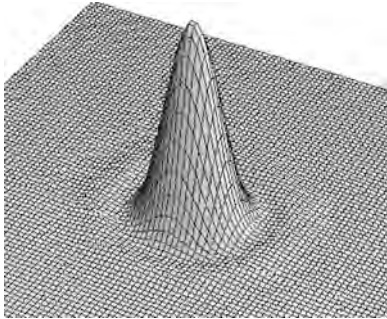


Figure 10 plots the Airy pattern of diffracted light from a point source imaged by a pinhole. The central lobe, called the Airy disc, totals 83.7% of the light falling on the image plane. All other light outside the first minimal ring contributes to diffraction fog.

Figure 11 plots the scanned digits from negatives taken in the pinhole camera with 180 sec exposures of the *4scaleW* and *4scaleB* targets.

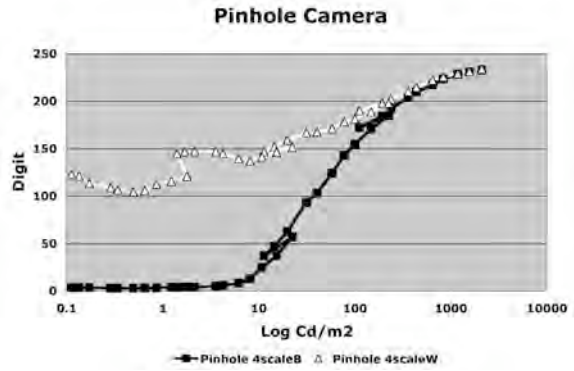


Figure 11 plots pinhole camera digits scanned from 800 ASA negative film images using 180 sec exposures.

The diffraction fog from the white surround increases responses of the gray sectors compared to the same luminances in the black surround. Figure 12 shows pinhole camera images compared to one of the digital pairs from Section 3.1. We selected the 180-second time with the pinhole camera to optimize exposures for both targets. The average digit for the highest luminance sector in Scale B [*4scaleBlack*- Pinhole] was 185. We selected the 1/8 sec digital image pair, because [*4scaleBlack*- Digital] had an average digit of 185 for the same sector.

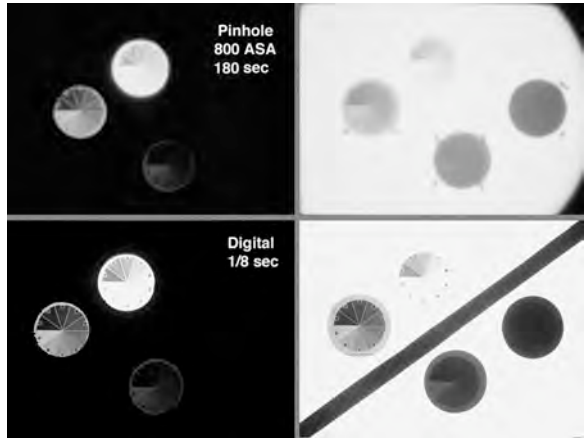


Figure 12 compares pairs of images made with the pinhole (without diagonal bar) and the digital camera. The pinhole images are less sharp and the *4scaleW* is lower in luminance range than the digital images.

Summarizing, regardless of the type of camera, film and lens, HDR images have strong optical limits. The range of light falling on the sensors is limited by veiling glare from parasitic images in glass lenses and diffraction fog in pinhole images. Although the glare is formed by reflections in one case, and diffraction in the other, they both show limited dynamic range. That range depends on both the both lens/camera and the scene. Scene dependence is a substantial problem for any ME2SL HDR algorithm²⁴ attempting to measure scene luminance.

4. VISUAL RESPONSE TO HDR DISPLAY

The second effect of veiling glare on HDR imaging is intraocular scatter that controls the dynamic range of luminances on the retina. In section 3.0 we saw that camera glare limits the range of luminances falling on the camera sensor plane. Human glare is caused by Tyndall scattering by macromolecules in the intraocular media, as well as the layers of neurons between the lens and the sensors. Scatter limits the eye's dynamic range more than glass lenses limit cameras. Here we will describe the range of discrimination and the corresponding range of retinal luminances. In addition, we will measure observed appearance for both *4scales Black* and *4scales White* test targets.

4.1 Visual Appearance of HDR Displays

We asked observers to evaluate the appearance of the *4scaleBlack* and *4scaleWhite* displays using magnitude estimation. Observers sat 1.9 m from the 61 cm wide display. The radius of each sector was 5.1 cm; subtending 2.4 degrees. Three observers were asked to assign 100 to the “whitest” area in the field of view, and 1 to the “blackest”. We then instructed them to find a sector that appeared middle gray and assign it the estimate 50. We then asked them to find sectors having 25 and 75 estimates. Using this as a framework the observers assigned estimates to all 40 sectors. The data from each observer (ages 31, 64, 68) was analyzed separately. No difference between observers was found.

The average magnitude estimate results (Figure 13) show very dramatically the role of spatial comparison and scattered light in vision. The *4scalesBlack* and *4scalesWhite* appearance estimates overlap for only the top 5 luminances. Below that, simultaneous contrast makes the luminances in the white surround darker. The white surround makes the local maxima in scales C and D darker than in the zero-luminance surround. Scattered light from the white surround severely limits all discrimination below 2 cd/m².

Min vs. Max Surrounds

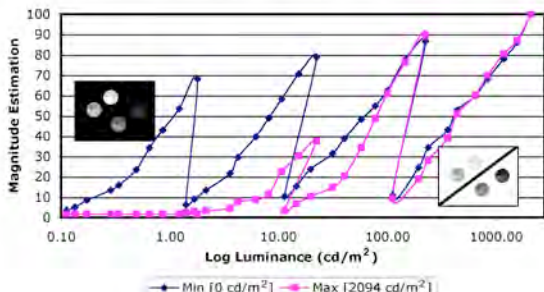


Figure 13 plots magnitude estimation of appearance vs. calibrated luminance for the 40 sectors in *4scalesBlack* and *4scalesWhite* test targets. Although the luminances are exactly equal the appearances are not. With a black surround observers can discriminate all 10 sectors in all four displays. With a white surround observers cannot discriminate below 2 cd/m².

The *4scalesBlack* estimates are very different from those in *4scalesWhite*. In *4scalesBlack*, the pie-shaped sectors with the highest luminance in each scale all appear light (Estimates: A=100, B=90, C=80, D=69). As shown in other experiments, the local maxima generate appearances that change slowly with luminance.²⁵ Nearby areas, with less luminance, change more quickly (physiological simultaneous contrast).

One can think of the *4scalesBlack* experiment as a 4-scale version of Land’s Black and White Mondrian²⁵. We have four different identical targets in four different illuminations. When the targets are isolated in the opaque surround we have three different examples of whites and blacks generated by the same luminances [(For 147 cd/m²; magnitude estimate = 17 in A and 87 in B), [(For 15 cd/m²; magnitude estimate =16 in B and 71 in C), [(For 1.8 cd/m²; magnitude estimate =10 in C and 68 in D)].

Also, we have four different luminances [1.06, 8.4, 63.5 and 414.] that generated the same appearance [ME= 50]. The same holds for all magnitude estimates except for the lightest and darkest. As argued in the original work,²⁶ there is no correlation of a pixel’s luminance with appearance. Models of appearance require a strong spatial component.

The opposite roles of physiological contrast and scattered light are seen in the difference appearances in white and black surrounds (Figure 13).²⁷ In the presence of white surrounds glare increases and appearances gets darker. These two targets change the amount of veiling glare, but do not measure the effect of glare because simultaneous contrast interferes. Different targets are necessary to understand the role of glare alone. We need pairs of targets that have constant contrast, but different dynamic ranges. Rizzi, Pezzetti, and McCann have studied single and double density targets with half-white and half-black surrounds.²⁸ The double density transparency target squares the dynamic range, yet has only a small effect on the magnitude estimates of appearance. Out of a possible range of 6.0 log units of display density, observers estimate that blacks are 3.0 log units darker than white. Additional range serves no purpose. Further, the 3.0 log range of luminances equals the range of conventional transparency film.

6. DISCUSSION

Veiling glare limits HDR imaging in two distinct ways. First, camera glare limits the luminance range that can be accurately measured (Section 3). Multiple exposures improve the quantization of digital records, but fail to accurately record scene luminance. Second, intraocular scatter limits the range of scene luminances falling on the retina (Section 4).

Accurate portrayal of scene luminances from camera images is both impossible to achieve and inessential to the visual process.

We were unable to make accurate camera estimates of scene luminance for the 4.3 log dynamic range scenes studied here. The comparison of white and black surrounds shows dramatic scene dependence. In addition, the camera flux estimates, when compared with actual flux, show a different error with each exposure. It may be tempting to look for some type of average-flux curve that represents data with smaller errors, but that idea is in conflict with the fundamental aim of the process, namely recording accurate scene luminance. Multiple-exposure HDR is limited by veiling glare that is scene-, exposure-, lens-, aperture-, and camera-dependent. The accuracy of scene-luminance estimates varies with all these parameters.

Some HDR algorithms attempt to correct for glare.^{29,30,31} Given the characteristics of the camera, they calculate the luminances in the scene. The glare spread functions of commercial lenses fall off very rapidly with distance to a very small value. We might think that such small glare values cannot affect distant pixels. However, there are millions of pixels that contribute glare to all other pixels. Each pixel is the sum of scene luminance plus scattered light from all other pixels. The sum of a very large number of small contributions is a large number. Sorting out these millions of scene-dependent contributions would be required to precisely correct for glare. ISO 9358:1994 Standard states unequivocally that: “the reverse [deriving luminance from camera response] calculation is not possible”⁹.

Claims are made that recent multiple-exposure HDR algorithms capture wider scene luminances, or colors than previously possible.³² These claims are severely limited by scene and camera veiling glare. As shown above, the designers of negative films selected a 4.1 log response range. That range exceeds the camera glare limit for almost all scenes.

Veiling glare for human vision is much worse than for cameras. Nevertheless, human vision has a much greater apparent dynamic range than camera systems. Humans can see details in highlights and shadows much better than conventional films and conventional electronic cameras can record. Although the rods and cones in the retina respond to more than a 10 log range, the ganglion cells that transmit the retinal response to the brain have only a 2 log range. There is no simple correlation between retinal quanta catch at a pixel and appearance.

The interplay between glare and physiological contrast is very complex. They act in opposition to each other, with physiological contrast tending toward canceling glare.²⁷ Since their mechanisms are so different, there is

no actual image-wise cancellation, as seen when a negative image is combined with a positive one, so that they make a uniform image. Intraocular glare, because it is the sum of contributions from all other pixels, adds a scene-dependent low-spatial-frequency mask to the scene. The effect of that mask is seen in the 4scalesWhite appearances. Discrimination is lost below 2 cd/m². By comparison, in 4scalesBlack with minimal glare observers can discriminate the entire 4.3 log range. Physiological contrast is a high-spatial frequency edge-based mechanism.^{33,34,35} The human visual system synthesizes images from edge information, using local maxima as a reference.²⁵ The local maxima in 4scalesBlack have estimates ranging over 100 to 69. Appearance below these maxima decrease rapidly with luminance. The physiological contrast based HVS image synthesis renders the four-level targets almost the same, despite large changes in luminances. Physiological contrast builds significant visual differences from small luminance differences on the retina. It is easy to understand that, if the surround around the 40 test sectors increases, then the glare increases, the magnitude of the luminance ratios at edges decreases, and physiological contrast makes the appearance of the smaller value darker. This counteraction of contrast and glare is fundamental to how we see. If the visual environment were only stars at night, then these low-glare scenes are easy to interpret because appearance tracks luminance.^{36,37,25} As scenes change from the starry night to grays-in-a-white-surround, glare decreases the edge ratios on the retina and physiological contrast increases relative differences in appearance.

Often we see discussions of HDR image capture in which dynamic range is equated to digital bit depth. Luminance and bit depth are equivalent only in a very special case that rarely happens. This case requires that the digits resulting from camera image plane luminances fall on a slope 1.0 plot with luminance. In the history of silver halide film, the only example of slope 1.0 is *slide duplication* film. Consumers do not like accurate (slope 1.0) pictures. Linear, slope 1.0, response functions are rare in digital cameras. The fundamental mechanism of CCDs tells us that the number of quanta caught is proportional to the charge in the pixel well. However, charge in a pixel is not linearly proportional to the output digit. There are anti-blooming (high luminances) and noise reduction (low luminances), and tone-scale functions built into most digital cameras. Digital output value cannot be assumed to be proportional to image plane luminance. A camera’s dynamic range is not equal to pixel bit depth. As shown above, the camera’s dynamic range has to be measured. The number of bits determines the number of quantization levels between max and min. The number of quantization levels determines whether two slightly different luminances are reproduced as different or the

same, which determines whether spatial detail in the scene is preserved or lost in the reproduction.

What is the mechanism that HDR capture and display uses to improve image reproduction? If not accurate records of luminance, what do multiple exposures accomplish? The luminous flux falling on the camera's image plane is the sum of the flux from the scene and the flux from glare. If we begin with an underexposed scene capture, we find scene information in the highlights, because the short exposure limits the absolute amount of glare. Here, there is insufficient flux to differentiate details in the shadows. Increasing the exposure to the best-average response does a good job of differentiating the mid-tone values. Increasing the exposure further, differentiates the details in the shadows while detail separation in the highlights is lost. Multiple exposures preserve spatial information over the range of luminances. It does not matter that we cannot unscramble the scene luminance from the scene flux and from flare flux.

Improved digital quantization, which allows discrimination of adjacent objects, can be used in spatial comparison algorithms. Unlike analog film density responses, digital imaging, particularly in the 1960's and 70's was limited to the number of bits available in electronic imaging devices. Although appropriately spaced 24 bits of data per pixel is close to being able to record the entire range detectable to human vision, it lacks the digital resolution to handle computations, such as de-mosaicing, image processing, printing and displaying a satisfactory picture. The number of bits, and more important, the luminance spacing between each bits is critical to having an artifact-free image.¹⁴ If digital cameras had photon well sizes and pixel digitizer circuits with 4.1 log range comparable to silver halide film, then multiple exposures would not be necessary. Such devices are too expensive for modern camera markets and have not been developed. Multiple exposures provide the mechanism to effectively increase the number of quantization levels that improves spatial discrimination of camera luminance data. Multiple exposures improve local information-- pixel A is darker than pixel B. That information is essential for synthesizing visual appearances of HDR scenes.

As discussed above, the significant role of intraocular glare has always prevented retinal receptors from seeing actual scene luminances. Physiological mechanisms, described as simultaneous contrast, work to reduce the adverse effects of glare. It follows that computational approaches to render HDR scenes for humans should use spatial comparisons as the essential tool in synthesizing the optimal display.^{1,38,39,40} The best approach to HDR is to follow the lead of artists' spatial rendering techniques, but with computational, rather than subliminal mechanisms.

7.0 CONCLUSIONS

This paper measures how much veiling glare limits HDR imaging in image capture and display. Glare is the scene- and camera- dependent scattered light falling on image sensors. First, glare limits the range of luminances that can be accurately measured by a camera, despite multiple exposure techniques. We used 4.3 log dynamic range test targets and a variety of digital and film cameras. In each case, the camera response to constant luminances varied considerably with changes in the surrounding pixels. HDR image capture cannot accurately record the luminances in these targets. Second, we measured the appearance of the same targets. Appearance did not correlate with luminance at a pixel: it depended on physical intraocular glare and physiological contrast.

The improvement in HDR images, compared to conventional photography, does not correlate with accurate luminance capture and display. Accurate capture in a camera is not possible, and accurate rendition is not essential. The improvement in HDR images is due to better preservation of relative spatial information that comes from improved digital quantization. Spatial differences in highlights and shadows are not lost. Spatial HDR image processing algorithms mimic processes developed by human vision, by chiaroscuro painters, and by early photographers that renders HDR scenes in low-range outputs.¹

ACKNOWLEDGEMENTS

The authors wish to thank S. Fantone, D. Orband and M. McCann for their very helpful discussions.

REFERENCES

*mccanns@tiac.net, rizzi@dti.unimi.it

¹ J. J. McCann, "Art, Science and Appearance in HDR Images", *J. SID Vol. 15(9)*, pp. in press 2007

² P. E. Debevec, J. Malik, "Recovering high dynamic range radiance maps from photographs", *ACM SIGGRAPH'97*, 369-378, 1997

³ H. Seetzen, W. Heidrich, W. Stuerzlinger, G. Ward, L. Whitehead, M. Trentacoste, A. Ghosh, and A. Vorozcovs, High dynamic range display systems (*ACM Transactions on Graphics*, Vol. 23(3)), 760-768, 2004

⁴ J. J. McCann and A. Rizzi, "Optical veiling glare limitations to in-camera scene radiance measurements", in *ECVP 2006 Abstracts, Perception*, Vol. 35, Supplement, p. 51, 2006

⁵ J. J. McCann and A. Rizzi, "Spatial Comparisons: The Antidote to Veiling Glare Limitations in HDR Images" in *Proc ADEAC/SID&VESA, Atlanta*, 155-158, 2006

⁶ J. J. McCann and A. Rizzi, "Veiling glare: the dynamic range limit of HDR images", in *Human Vision and Electronic Imaging XII*, eds. B. Rogowitz, T. Pappas, S. Daly, Proc. SPIE, Bellingham WA, 6492-41, 2007

⁷ J. J. McCann and A. Rizzi, "Spatial Comparisons: The Antidote to Veiling Glare Limitations in Image Capture and

Display” Proc. IMQA 2007, Chiba, E-1, 2007

⁸ The term *contrast* has different definitions in photography and vision. In photography, it refers to the rate of change in reproduction luminance vs. scene luminance. It is the slope of the tone-scale function. In vision, it is the name of the spatial mechanism that enhances differences in appearance. A gray patch in a white surround is darker because of the physiology in the visual system, referred to as simultaneous contrast.

⁹ ISO 9358:1994 Standard, “Optics and optical instruments. Veiling glare of image forming systems. Definitions and methods of measurement”, (ISO, 1994)

¹⁰ J. W. Gillon, U.S. Patent, 2,226,167, December 4, 1940

¹¹ S. Ochi and S. Yamanaka, US Patent, 4,541,016, filed Dec 29, 1982, issued Sep 10, 1985

¹² L. E. Alston, D. S. Levinstone, W. T. Plummer, “Exposure control system for an electronic imaging camera having increased dynamic range”, US Patent 4,647,975, Filing date: Oct 30, 1985, Issue date: Mar 3, 1987

¹³ S. Mann, Compositing Multiple Pictures of the Same Scene”, Proc. IS&T Annual Meeting, Vol. **46**, pp. 50-52, 1993

¹⁴ S. Mann and R. W. Picard, “On Being “Undigital” with Digital Cameras: Extending Dynamic Range by Combining Different Exposed Pictures”, Proc. IS&T Annual Meeting, Vol. **48**, 442-448, 1995

¹⁵ J. J. McCann, “Calculated Color Sensations applied to Color Image Reproduction”, in *Image Processing Analysis Measurement and Quality*, Proc. SPIE, Bellingham WA, Vol. **901**, pp. 205-214, 1988

¹⁶ L. A. Jones and H. R. Condit, “The Brightness Scale of Exterior Scenes and the Computation of Correct Photographic Exposure”, *J. Opt. Soc. Am.*, Vol. **31**, pp. 651-678, 1941

¹⁷ C. E. K. Mees, *Photography*, (The MacMillan Company, New York, 1937)

¹⁸ C. E. K. Mees and T.H. James, *The Theory of the Photographic Process*, 3rd ed., (The MacMillan Company, New York 1966).

¹⁹ A. L. M. Sowerby, *Dictionary of Photography*, 18th edition, (Philosophical Library, New York, 1956), p. 568

²⁰ The formula to count parasitic images (π_i) is: $\pi_i = 2n^2 - n$, where n is the number of lenses.¹⁹

²¹ This question was raised by Jim Larimer, (personal communication).

²² P. Padley, ‘Diffraction from a circular aperture’, <<http://cnx.org/content/m13097/latest/>>

²³ R. W. Ditchburn, “Light”, (Dover, New York, 1991) p. 165

²⁴ E. Reinhard, G. Ward, S. Pattanaik, P. Debevec, *High Dynamic Range Imaging Acquisition, Display and Image-Based Lighting*, (Elsevier, Morgan Kaufmann, Amsterdam, chap 6-7, 2006)

²⁵ J. J. McCann, “Aperture and Object Mode Appearances in Images”, in Human Vision and Electronic Imaging XII, Eds. B. Rogowitz, T. Pappas, S. Daly, Proc. SPIE, Bellingham WA, Vol. **6292-26**, 2007.

²⁶ E. Land and J. J. McCann, “Lightness and Retinex Theory”, *J. Opt. Soc. Am.*, Vol. **61**, pp. 1-11, 1971.

²⁷ J. J. McCann, “Spatial Contrast and Scatter: Opposing Partners in Sensations”, in Human Vision and Electronic Imaging IV, B. Rogowitz and T. Pappas, Eds., SPIE Proc., Vol. **3644**, pp. 97-104, 1999

²⁸ A. Rizzi, M. Pezzetti, and J. J. McCann, “Intraocular glare controls the visible range of High Dynamic Range Images (HDRI)”, Proc IS&T/SID Color Conference, 2007.

²⁹ F. Xiao, J. M. DiCarlo, P. B. Catrysse and B. A. Wandell, “High Dynamic Range Imaging of Natural Scenes” Proc

IS&T/SID Color, Vol. **10**, 337-342, 2002

³⁰ E. Reinhard, G. Ward, S. Pattanaik, P. Debevec, *High Dynamic Range Imaging Acquisition, Display and Image-Based Lighting*, Elsevier, Morgan Kaufmann, Amsterdam, chap 4, 2006.

³¹ B. Bitlis, P. A. Jansson, and J. P. Allebach “Parametric point spread function modeling and reduction of stray light effects”, in *Computational Imaging V*, eds. C. Bouman, E. Miller & I. Pollak, Proc. SPIE, Bellingham WA, **6498-27**, 2007.

³²<<http://www.cs.nott.ac.uk/%7Equi/jvci/Call-for-Papers.html>>

³³ V. O’Brien, “Contrast by contour-enhancement”, *Am J Psychol*, Vol. **72**, pp. 299–300, 1959

³⁴ T. Cornsweet, *Visual Perception*, (New York: Academic Press, 1970).

³⁵ E. H. Land, “Smitty Stevens’ Test of Retinex Theory” in *Sensation and Measurement Papers in Honor of S. S. Stevens*, (Applied Science Publishers, Ltd., London, 1974) pp. 363-368

³⁶ J. J. McCann, “Rendering High-Dynamic Range Images: Algorithms that Mimic Human Vision”, in Proc. AMOS Technical Conference, Maui, pp. 19-28, 2005.

³⁷ H. Takahashi, H. Yaguchi and S. Shiori, “Estimation of Brightness and Lightness in All Adaptation Levels”, *J. Light & Vis. Env.* Vol. **23**, pp. 38-48, 1999.

³⁸ J. J. McCann, “Capturing a Black Cat in Shade: The Past and Present of Retinex Color Appearance Models”, *J. Electronic Img* Vol. **13**, pp. 36-47, 2004.

³⁹ A. Rizzi, C. Gatta, D. Marini, “A New Algorithm for Unsupervised Global and Local Color Correction”, *Pattern Recognition Letters*, Vol. **24**, No. 11, July 2003, pp. 1663-1677.

⁴⁰ J.J. McCann, ed., “Retinex at Forty”, *J. Electronic Img*, Vol. **13**, pp.1-145, 2004.